Eur. Phys. J. D **9**, 21–24 (1999)

THE EUROPEAN PHYSICAL JOURNAL D

EDP Sciences

Angular distributions in photoelectron spectroscopy of small tungsten clusters: competition between direct and thermionic emission

J.C. Pinaré, B. Baguenard, C. Bordas, and M. Broyer

Laboratoire de Spectrométrie Ionique et Moléculaire, Université Claude Bernard, Lyon 1 and CNRS, Bât. 205 43, Boulevard du 11 Novembre 1918, F-69622 Villeurbanne Cedex, France

Received: 2 September 1998

Abstract. Single-photon photodetachment of mass-selected W_n^- clusters has been studied by velocity map imaging. Photoelectron imaging allows us to measure simultaneously the kinetic energy spectrum and the angular distribution of photoelectrons, providing a clear distinction between the isotropic thermionic emission and the anisotropic direct photoemission. A careful study of threshold electrons shows that the thermal distribution $p(\epsilon)$ cannot be described, even qualitatively, by a simple exponentially decreasing Boltzmann function, as is usually assumed. On the contrary, our results are in excellent agreement with more refined theoretical models. Our results indicate that the transition towards a bulk-like statistical behavior of the internal energy redistribution occurs in very small systems, because of the high density of states in metal clusters. The asymmetry parameter β of the most intense band observed in direct photoemission for each cluster decreases monotonically with size; the direct photoemission of small systems is strongly anisotropic, and becomes isotropic as the size of the system increases. This probably indicates the loss of coherence induced by electron–electron collisions occurring in large systems prior to electron–phonon coupling.

PACS. 36.40.-c Atomic and molecular clusters – 33.60.Cv Ultraviolet and vacuum ultraviolet photoelectron spectra

1 Introduction

In a complex system such as a cluster or solid, the absorption of one or several photons results in electronic excitation which, at least partly, may be transferred to the nuclei by electron–phonon couplings, leading to a significant increase of the internal temperature of the system. If one neglects the initial temperature, the internal temperature T of a system containing N particles after absorption of a photon of energy $h\nu$ may be expressed as:

$$T = \frac{h\nu}{(3N-6)k_{\mathrm{B}}} \tag{1}$$

with k_{B} the Boltzmann constant. In a small cluster, this temperature may be extremely high. For example, the absorption of a 4 eV photon by a cluster containing 4 atoms leads to an internal temperature close to 8000 K. At this temperature, the excited system may decay by emission of an electron or an atom, and the kinetic energy spectrum of the emitted particle is a precise probe of the internal thermal excitation. This phenomenon is particularly interesting in clusters of refractory compounds where the energy required to remove an electron is significantly lower than the energy required to remove an atom. The hot refractory clusters may thus decay only by electronic emission. Negative clusters of refractory elements such as tungsten [1–6], niobium [7] or fullerenes [8–12] have already been studied by single- or multi-photon ionization followed by time-of-flight mass spectrometry or by photoelectron spectroscopy.

In this paper, we focus on the case where the absorption of a single photon of energy $h\nu$ is sufficient to remove an electron from a finit-size negatively charged system: $h\nu > \mathrm{EA}$ (electron affinity). As model systems, we study the photodetachment of W_n^- clusters ($n < 12$) by single-photon excitation. Small negative tungsten clusters W_n^- may be considered as the prototypes of refractory systems since their electron affinity is less than 2 eV [4], while the bulk heat of vaporization is about 8.9 eV/atom. Neutral [1–3] and negative [4–6] tungsten clusters have already been extensively studied and the kinetic-energy distribution of photoelectrons has been measured [4–6] using a magnetic bottle photoelectron spectrometer [13]. As opposed to standard techniques, our photoelectron imaging spectrometer allows us to study the photoelectron spectrum near threshold where it is expected to be extremely different in a finite-size system and in bulk matter. Two processes dominate the decay of the hot clusters. First, the excited state can lead directly to the emission of a photoelectron. This corresponds to direct photoemission (DPE): the excess energy is converted to photoelectron kinetic energy $\epsilon = h\nu - E_{\mathrm{f}}$ (E_{f} energy of the final state of the target). In that case, the kinetic energy photoelectron spectrum

mirrors the target excited-state spectrum. Second, before direct decay, the excited electron may transfer part of its energy to the nuclei. In bulk matter, this results in inelastic photoelectron scattering [14], while in clusters, because of the combination of a limited number of degrees of freedom and a large density of states, this indirect process leads to a significant increase of the internal temperature, which results in thermionic emission (TE) [15].

In bulk matter, TE corresponds to the ejection of electrons from a surface at temperature T with a kinetic energy distribution described by:

$$p(\epsilon) \propto \epsilon \times \exp(-\epsilon/k_{\mathrm{B}}T). \quad (2)$$

The bulk-like function (2) is not relevant to finite size systems. The detailed theoretical aspects of TE of clusters has been extensively studied by Klots and co-workers [16, 17]. According to [16], the kinetic energy distribution of TE of a cluster of N atoms of radius R_N ($R_N = r_s N^{1/3}$ with r_s the Wigner–Seitz radius) may be expressed as:

$$p(\epsilon) \propto \left[1 - \exp\left(-BL^2_{\max}(\epsilon)/k_{\mathrm{B}}T\right)\right] \times \exp(-\epsilon/k_{\mathrm{B}}T) \quad (3)$$

where the maximum value of the angular momentum $L_{\max}$ of the outgoing electron may be written, for a negatively charged system, as

$$L^2_{\max}(\epsilon) = \frac{2\mu}{\hbar^2}\left[\left(2\alpha e^2 \epsilon\right)^{1/2} + \epsilon R_N^2 + \cdots\right], \quad (4)$$

and for a neutral or positively charged system, as

$$L^2_{\max}(\epsilon) = \frac{2\mu}{\hbar^2}\left[e^2 R_N + \epsilon R_N^2 + \cdots\right], \quad (5)$$

with μ and e the mass and charge of the electron, respectively, and α the static polarizability of the cluster. Because of the low mass of the electron, (3) may be rewritten as:

$$p(\epsilon) \propto L^2_{\max}(\epsilon) \times \exp(-\epsilon/k_{\mathrm{B}}T). \quad (6)$$

These equations show that the photoelectron spectra of negative clusters differ significantly from the spectra of neutral or positive clusters. This difference arises from the fact that in the case of a negative cluster, the residual interaction between the core and the outgoing electron is dominated by a polarization long-range potential, while for a neutral or positive cluster, this interaction is a Coulomb potential. In the limit of small particles ($R_N \to 0$), the dominant contribution to $p(\epsilon)$ is proportional to $\left(\epsilon^{1/2} \times \exp(-\epsilon/k_{\mathrm{B}}T)\right)$ in photodetachment and to $\exp(-\epsilon/k_{\mathrm{B}}T)$ in photoionization. For a given temperature T, the maximum of $p(\epsilon)$ is found at $\epsilon_0 \approx \frac{1}{2}k_{\mathrm{B}}T$ in photodetachment of a small negative cluster, while $p(\epsilon)$ is maximum at $\epsilon_0 \approx k_{\mathrm{B}}T$ in bulk matter. The energy spectrum of thermal electrons ejected by a finite-size negatively charged system is thus shifted toward lower energies, as compared to bulk matter at the same temperature T. In this paper, we present the first experimental results showing without ambiguity the specific behavior of TE of small negative clusters.

2 Experimental results and discussion

In order to distinguish kinetic energy distributions of the form described by (2) or by (3) and (4), low-energy electrons (typically $\epsilon < 0.2$ eV) must be detected with the same efficiency as fast electrons. From this point of view, standard techniques, such as the magnetic bottle spectrometer [13], are not appropriate. Instead, we use an improved photoelectron imaging technique, namely velocity map imaging [18, 19]. Our experimental setup is as follows. Metal clusters (neutrals or ions) are produced in a laser vaporization source seeded with helium. The internal temperature of the clusters is estimated below 300 K. Native anions are extracted from the cluster beam in the extraction region of a time-of-flight mass spectrometer (TOFMS) by a pulsed electric field. The photoelectron imaging spectrometer [20–22] is located at the end of the TOFMS. An adjustable delay between the extraction pulse and the photodetachment laser (λ=308 nm) allows the excitation of a well-defined cluster size. All photoelectrons produced in the photodetachment process are projected onto a position-sensitive detector. Experimental images are recorded via a digital CCD camera. After inversion [22], the initial energetic and angular distribution of the photoelectrons may be extracted from the experimental image.

Figure 1 presents typical photoelectron images of W_4^-, W_6^-, W_8^-, and W_{11}^- at $\lambda = 308$ nm under equal experimental conditions. All images exhibit two qualitatively different main features. First, there is a broad and isotropic central peak, corresponding to slow electrons, that can be attributed to TE. The precise observation of this distribution relies entirely on the fact that imaging techniques have a linear efficiency near threshold. This broad distribution is surrounded by sharper structures, not necessarily isotropic (usually more intense along the laser polarization axis for low n values), corresponding to DPE. Indeed, in DPE, the photoelectron angular distribution depends on the angular couplings in the initial and final states of the target and is usually anisotropic while in TE; the initial orientation is lost during the internal energy redistribution process, and the thermal electron emission is isotropic. The ability to resolve angular distribution is thus a direct means of discriminating between the various decay processes. Photoelectron spectra obtained after image inversion are displayed in Fig. 2 for W_n^- clusters with $n = 4-11$ (bold line).

Distributions calculated in the bulk-like limit (dashed line – (2)) and according to Klots' formula (thin solid line – (3) and (4)) are compared with experimental results. In the low-energy range (0–0.5 eV), a contribution described by (3) and (4) accounts for the major part of the spectrum, while the bulk formula predicts a distribution slightly shifted towards higher energy. The agreement is particularly spectacular for larger sizes ($n = 8-11$) but is also surprisingly good in small systems such as W_4^-. Since the cluster is initially cold, the simplest expression (1) has been used for the temperature T as an approximation of the isokinetic temperature [16]. The static polarizability is taken to be $\alpha = R_N^3$. The remaining part of the spectrum is the contribution from DPE, which corresponds essen-

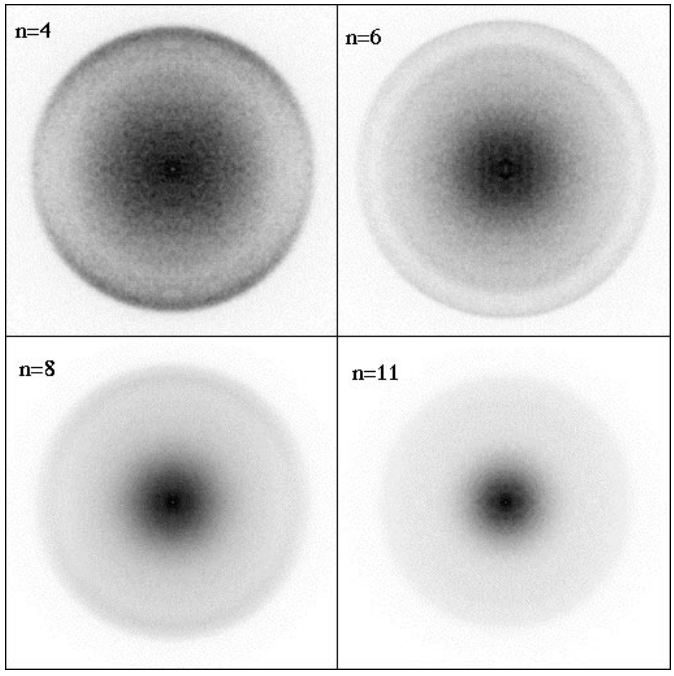

Fig. 1. Typical photoelectron images of W_n^- clusters ($n = 4$, 6, 8, and 11) at $\lambda = 308$ nm. All images are recorded under the same experimental conditions. Laser polarization is oriented along the vertical axis. The intensity scale ranges from 0% (white) to 100% (black) of maximum intensity. The isotropic slow thermal electron distribution is visible in the center of the image; its narrowing with increasing size n is clearly visible. It is surrounded by anisotropic and sharper features corresponding to direct photoemission.

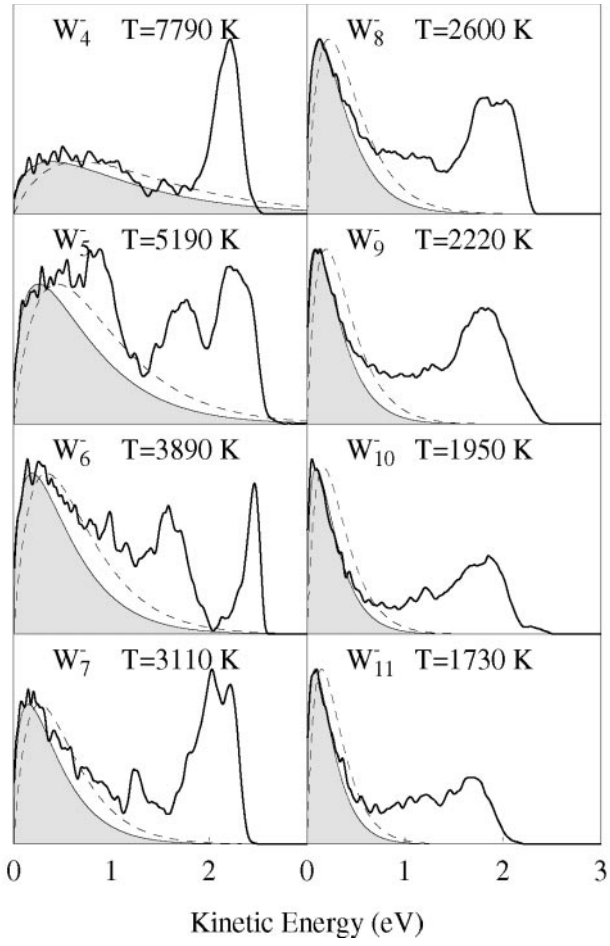

Fig. 2. Photoelectron kinetic energy spectrum obtained after image inversion for W_n^- clusters with $n = 4-11$ (broad solid line). The contribution of TE $(2-4)$ is plotted by a thin solid line (light-gray filled). The dashed line corresponds to the bulk limit at the same temperature T (1). Below 0.5 eV, the agreement between experiment and Klots' formula is remarkable. The remaining part of the spectrum is the contribution of direct photoemission.

tially to the building up of the d-valence band of tungsten. Our experiments have been conducted under low laser fluence in order to avoid multiphoton processes. Photoelectron spectra are recorded in the linear regime where the shape of the whole spectrum does not depend on the laser fluence.

The branching ratios between TE and DPE may be extracted from the experimental data. The ratio $\rho_{\mathrm{TE}} = I_{\mathrm{TE}}/I_{\mathrm{total}}$ is plotted in Fig. 3. In the range $n = 4-11$, both decay processes are of comparable magnitudes ($\rho_{\mathrm{TE}} \approx 0.5$), as reported in previous experiments [5]. This is rather surprising since ρ_{TE} vanishes in the small-size limit: only DPE occurs in atoms and dimers. Similarly, the Richardson–Dushman law [15] predicts that the absolute rate of TE is proportional to $T^2 \exp(-W/k_{\mathrm{B}}T)$ [15]. Since T decreases with the cluster size, like n^{-1}, one would expect also a significant decrease of the ratio ρ_{TE} at large n values. We attribute the roughly constant value of the ratio ρ_{TE} in large clusters to the stronger electron–phonon couplings induced by the increasing number of vibrational degrees of freedom. Measurement of absolute rate for TE and DPE are required in order to clarify this point.

One of the main advantages of imaging techniques is that they provide simultaneously the angular and kinetic energy distribution. As already mentioned, this capability allows one to discriminate easily between a direct process such as DPE, which usually leads to anisotropic distributions, and an indirect process like TE, which leads to a totally isotropic distribution. More quantitatively, the anisotropy of the photoelectron distribution in a given energy range is measured by the asymmetry parameter β [23], defined as:

$$I(\theta) = \frac{\sigma_{\mathrm{total}}}{4\pi}\left[1 + \beta P_{20}(\cos\Theta)\right], -1 \leq \beta \leq 2 \qquad (7)$$

with Θ the angle between the laser polarization axis and the direction of ejection of the electron, and the Legendre polynomial $P_{20}(\cos\Theta) = \frac{3}{2}\cos^2\Theta - \frac{1}{2}$. The asymmetry parameter β of the most intense band observed in DPE is plotted in Fig. 3 for each cluster size. The general trend in the evolution of this parameter is a monotonic decrease with n. The DPE of small systems is strongly anisotropic, and is aligned along the laser polarization axis ($\beta \approx 1$). It becomes more isotropic as the size of the system increases ($\beta \to 0$). The parameter β is closely related to the angu-

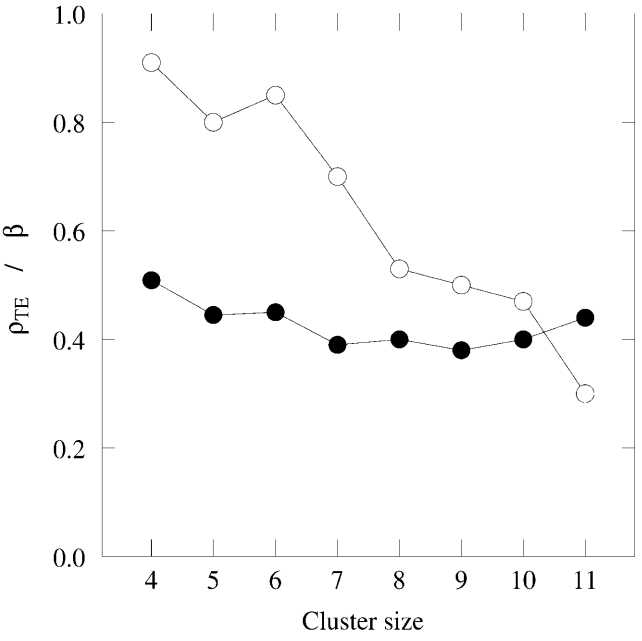

Fig. 3. Branching ratio $\rho_{\mathrm{TE}} = I_{\mathrm{TE}}/I_{\mathrm{total}}$ (•) and asymmetry parameter β (○) of the most intense band observed in DPE, as a function of cluster size. In the range $n = 4-11$, both decay processes are of comparable magnitudes ($\rho_{\mathrm{TE}} \approx 0.5$). The DPE of small systems is strongly anisotropic and is aligned along the laser polarization axis ($\beta \approx 1$). It becomes more isotropic as the size of the system increases ($\beta \to 0$).

lar correlations occurring in the photodetachment process. In other words, β depends on the radial and angular properties of the wave function of the initial and final states of the system. Angular correlations in metal clusters containing a large number of free electrons are extremely difficult to analyze, and are beyond the scope of the present paper. However, it is very unlikely that a direct photoionization or photodetachment process in a complex system leads to a totally isotropic emission, as is observed in the present case at large n values. Therefore, we assume that the observed structures attributed to the building up of the d-valence band of tungsten do not strictly correspond to direct photoemission. Rather, we interpret the rapid decrease of β as an indication of the loss of coherence induced by electron–electron collisions occurring in large systems prior to electron–phonon couplings.

3 Conclusion

The use of photoelectron imaging spectroscopy to study the photodetachment of mass-selected clusters was initially motivated by the high resolution of imaging techniques near threshold. However, our observation of TE as the dominant process in the low-energy range demonstrates that high-resolution threshold photoelectron spectroscopy of such clusters is not achievable. Indeed, photodetachment just above threshold results in a continuous thermal distribution, and does not allow high-resolution spectroscopy. Our careful study of the kinetic energy distribution of threshold electrons shows that the thermal distribution cannot be described by a simple bulk-like exponential formula. On the contrary, our results are in excellent agreement with the more refined model developed by Klots [16]. Moreover, our results indicate that the transition towards a bulk-like statistical behavior of the internal energy redistribution occurs even in very small systems ($n \geq 4$), because of the high density of states in metallic clusters.

The Laboratoire de Spectrométrie Ionique et Moléculaire is an Unité Mixte de Recherche CNRS-Université Lyon I (UMR CNRS 5579).

References

1. A. Amrein, R. Simpson, P. Hackett: J. Chem. Phys. **94**, 4663 (1991)
2. A. Amrein, R. Simpson, P. Hackett: J. Chem. Phys. **95**, 1781 (1991)
3. T. Leisner, K. Athanassenas, D. Kreisle, E. Recknagel, O. Echt: J. Chem. Phys. **99**, 9670 (1993)
4. H. Weidele, D. Kreisle, E. Recknagel, G. Shulze Icking-Konert, H. Handschuh, G. Ganteför, W. Eberhardt: Chem. Phys. Lett. **237**, 425 (1995)
5. G. Ganteför, W. Eberhardt, H. Weidele, D. Kreisle, E. Recknagel: Phys. Rev. Lett. **77**, 4524 (1996)
6. H. Weidele, S. Becker, H.J. Kluge, M. Lindinger, L. Schweikhard, C. Walther, J. Ziegler, D. Kreisle: Surf. Rev. Lett. **3**, 541 (1996)
7. B.A. Collings, A.H. Amrein, D.M. Rayner, P.A. Hackett: J. Chem. Phys. **99**, 4174 (1993)
8. L.S. Wang, J. Conceicao, C. Jin, R.E. Smalley: Chem. Phys. Lett. **182**, 5 (1991)
9. E.E.B. Campbell, G. Ulmer, I.V. Hertel: Phys. Rev. Lett. **67**, 1986 (1991)
10. Y. Zhang, M. Stuke: Phys. Rev. Lett. **70**, 3231 (1993)
11. J.U. Andersen, C. Brink, P. Hvelplund, M.O. Larsson, B. Bech Nielsen, H. Shen: Phys. Rev. Lett. **77**, 3991 (1996)
12. K. Hansen, O. Echt: Phys. Rev. Lett. **78**, 2337 (1997)
13. P. Kruit, F.H. Read: J. Phys. E **16**, 313 (1983)
14. G. Ertl, J. Küppers: *Low Energy Electrons and Surface Chemistry* (VCH Verlagsgesellschaft, Weinheim 1985)
15. N.W. Ashcroft, N.D. Mermin: *Solid State Physics*, ed. by Saunders College, Philadelphia (London 1976)
16. C.E. Klots: J. Chem. Phys. **90**, 4470 (1989); Z. Phys. D **20**, 105 (1991); Chem. Phys. Lett. **186**, 73 (1991); J. Chem. Phys. **98**, 1110 (1993); J. Chem. Phys. **100**, 1035 (1994)
17. C.E. Klots, R.N. Compton: Surf. Rev. Lett. **3**, 535 (1996)
18. D.H. Parker, A.T.J.B. Eppink: J. Chem. Phys. **107**, 2357 (1997)
19. A.T.J.B. Eppink, D.H. Parker: Rev. Sci. Instrum. **68**, 3477 (1997)
20. H. Helm, N. Bjerre, M. Dyer, D. Huestis, M. Saeed: Phys. Rev. Lett. **70**, 3221 (1993)
21. C. Bordas, M.J. Dyer, T. Fairfield, H. Helm, K.C. Kulander: Phys. Rev. A **51**, 3726 (1995)
22. C. Bordas, F. Paulig, H. Helm, D.L. Huestis: Rev. Sci. Instrum. **67**, 2257 (1996)
23. H.A. Bethe, E.E. Salpeter: *Quantum Mechanics of One-Electron Atoms* (Springer-Verlag, Berlin 1957)